Numerical Investigation of Compressor Tandem Aerofoils Featuring Near-Endwall Modification

Numerical Investigation of Compressor Tandem Aerofoils Featuring Near-Endwall Modification

J Eckel[1] and V Gümmer[1]

[1] Chair of Turbomachinery and Flight Propulsion, TUM Department of Mechanical Engineering, Technical University of Munich, Boltzmannstraße 15, 85748 Garching, Germany

jannik.eckel@ltf.mw.tum.de and volker.guemmer@ltf.mw.tum.de

Abstract. A highly loaded 1.5-stage low-speed compressor stage is investigated numerically using fully turbulent and steady state RANS simulations. The tandem stator at the end of the stage is replaced by a tandem stator with a near-endwall modification. This unconventional compressor blade design is using a single profiling near both endwalls and a tandem profiling at midspan. Using this modification the positive behaviour of a tandem stator can be maintained. Locally the leading edge of the rear vane and as a result the gap flow near both endwalls will be removed by introducing a single-profile segment. This paper will describe the approach to set up a numerical model for the new geometry and will characterize the flow features and loss mechanisms of the near-endwall modification. The first comparison between the stators with and without near-endwall modification, showed a reduction of corner separation at the rear vane, caused by the removal of the low momentum gap-flow. On the other side, the near-endwall modification is creating higher losses at the connecting region between the tandem and single segment. The numerical results presented in this paper will be the starting point for further optimizations of the tandem blade with near-endwall modifications.

1. Introduction

The design and investigation of highly loaded compressors with large pressure ratios is one of the major objectives of modern aircraft design. Based on performance studies high overall compressor pressure ratios will increase the thermal efficiency and reduce the specific fuel consumption of the entire aero engine [1]. The major challenge for such highly loaded compressors are the additional requirements of a light and short geometry of the compressor, which proposes to avoid the use of a big amount of stages to achieve the required pressure ratio. Based on this approach every stage of the compressor has to achieve a higher stage loading. For conventional blade designs, this implies an increase in flow tuning over each blade passage such as a higher diffusion. Both effects will lead to stronger secondary flow phenomena like the corner separation, which is limiting the maximum pressure rise and working range of each stage [2]. Based on these statements the blading of modern compressors is facing the challenge to gain high loadings, a wide working range and at the same time good efficiencies. Classical blade designs are facing their limits under these requirements. The tandem blade is an older approach to achieve higher pressure ratios and a wider working range due to the use of a two blades that are placed in short axial and circumferential distance to each other [3]. Numerical and experimental research of the last years showed that the tandem blade design is able to provide higher flow turnings compared to conventional single blade designs but still faces some challenges. The major challenges are the higher

secondary flow losses of the tandem blade at design conditions, which are mainly linked to the existence of the second leading edge of the rear vane [4]. The introduction of the new tandem stator with a near-endwall modification is one possible way to master the challenge of the tandem blade by geometrical removing the second leading edge of the rear vane.

2. Description and creation of the near-endwall modification

The tandem stator with near-endwall modification (figure 1) consists of a tandem-profile segment that is placed between two single-profile segments with only one blade profile. The single-profile segments are coupled to the hub and shroud surfaces and form the near-endwall modification and the connecting regions. The geometry of a preliminary designed reference tandem stator is the input for the tandem- and single-profile segment. Because of this approach, it is possible to achieve the same metal angles at the leading (LE) and trailing edge (TE) of the geometry with and without near-endwall modifications, which is a one of the constraints of the new design. Another constraint is the avoidance of overlapping edges near the so-called connecting regions. The connecting regions are the areas where the single-profile segments are linked to the tandem-profile segment. The structure of those regions has to eliminate the existence of unnecessary gaps und sharp edges. The last requirement is the removal of the second

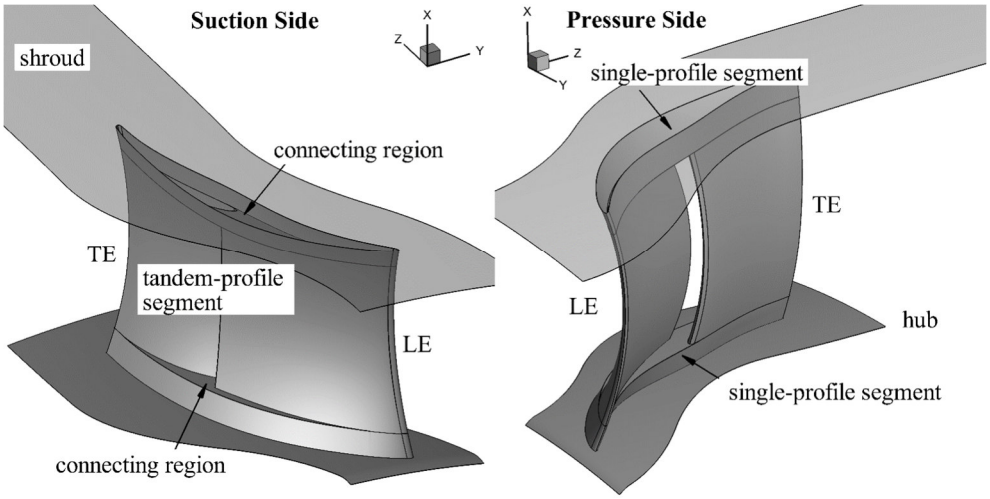

Figure 1. 3D-geomtry of a tandem stator with near-endwall modification

leading edge of the rear vane. This goal is achieved automatically by the near-endwall modification due to the single profiling of the blade sections near hub and shroud. The simplified process chain that is providing the geometry data for the numerical set up is shown in figure 2. The specification of the input data represents the first step of the algorithm and includes the transfer of parametrization data for each single-profile segment and the geometrical coordinates (x, y and z) of the reference tandem stator. The second step of the algorithm is the geometry preparation process. First, an adaption of the point distribution of each blade section, an extrusion of the blade and an increase of the number of blade sections is performed for the input geometry. This is important for an improved surface and grid generation of the later steps. Second, the parametrization data of the near-endwall modification, for example the relative height of each single-profile segment or the profiling of the single-profile segments are used to calculate the new geometry points. In contrast to a classical blade design, the profiles of the single-profile segment cannot be defined by for example a double circular arc or NACA profile. The reason for a more complex approach is the constraint of the enveloping profile at the connecting region, which cannot be achieved by a classical profile without changing the profiling of reference tandem stator. The parametrization of a profile for the single-profile segment at the connecting region can be seen in figure 2. The profile is defined by four control points (CP), which are determining the beginning

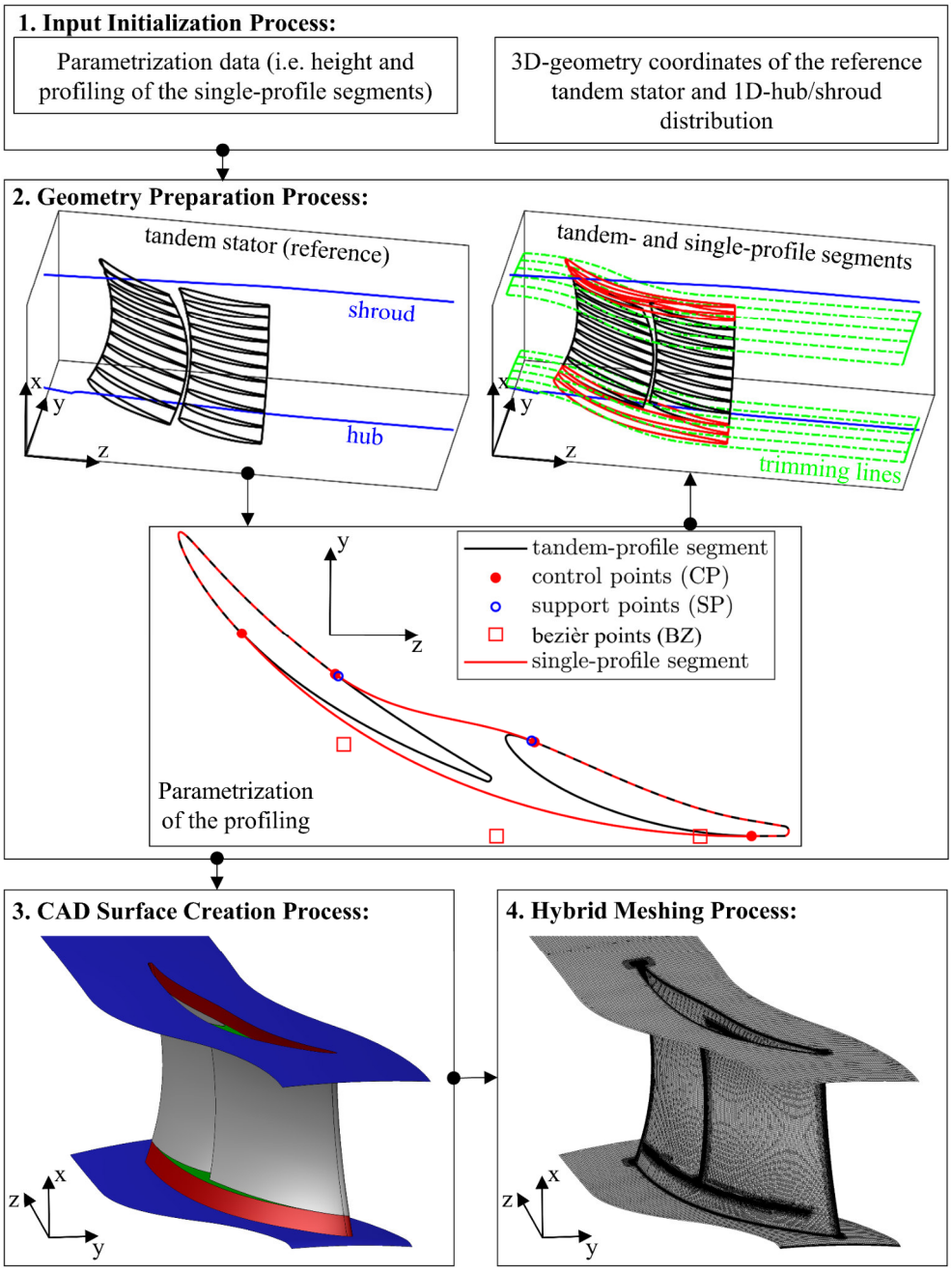

Figure 2. Process chain of the generation of a tandem stator with near-endwall modification

and the end of the link between the front and the rear vane. The shape of the suction side is calculated by a bezièr approach that is using five bezièr points (BZ). Two of the five bezièr points are the control points themselves, which are providing a C^0 continuity between the profile of reference and single-profile segment. Two other Bezièr points near the connecting points are placed relatively to them. Moreover, the tangential position of those Bezièr points is dependent of the local curvature of the reference profile at the connecting points. This approach reduces the number of free parameters, helps to achieve a C^1 continuity near the connecting points and averts crossing points of the profile of the single-profile segment with the reference profile. The fifth Bezièr point can freely be set to manipulate

the shape the new profile. Based on this method the curvature and the thickness of the single-profile segment highly depends on the position of the control point at the front vane. For example, a small relative axial position of the first control point will produce a thicker single-profile segment in contrast to a control point that is placed near the trailing edge of the front vane. The pressure side of the single-profile segment is using two support and two control points for a cubic spline interpolation implemented in Matlab™. The reason for the different approach of the pressure side is the fact that the near-endwall modification needs to create an enveloping geometry around the reference geometry with no overlapping edges. A cubic spline interpolation using those four points is able to create a robust and smooth profile for the pressure side with a minimal necessary increase of blade thickness, which is also able to evade around the leading edge of the rear vane. The retention of the geometrical points between the connecting points and the leading respectively trailing edges of the reference profile allows keeping the geometrical turning of each section constant in comparison to the turning of the reference tandem stator. One additional feature of the single-profile segment is the integration of tiny ramps at each connecting point. Without those ramps the resulting connecting surfaces would poses angles near zero at the connecting points, which will create highly distorted cells during the unstructured grid generation process. After the profiling is done the parameter of the relative height of the single-profile segment is used to calculate axisymmetric trimming lines, which are defining the connecting region and are separating the tandem-profile segment from the single-profile segment.
After the geometry preparation process is finished the point cloud of the single-profile segments, the reference tandem stator and the trimming lines are transferred to the commercial CAD software CatiaV5™, which is used to construct the surface model and the fluid domain. The CAD process uses program specific multi-section surface, intersection, joining and splitting functions to create the geometry of the whole blade row.
The commercial unstructured grid generation software HexpressHybrid™ does the meshing of the tandem stator with near-endwall modification during the last step of the process chain. The isotropic and hybrid meshing approach has to be used due to the complex geometries at the connecting regions.

3. Numerical set up and grid study

The investigation of the tandem stator with near-endwall modification is performed inside the environment of a preliminary design 1.5-stage compressor (figure 3). The reference tandem stator (row 3) at the end of the original compressor can be replaced by the modified geometry. Figure 3 shows the use of rotor-stator interfaces (RSI) between all rows of the compressor, which are utilizing the 1-D non-reflecting mixing plane approach [5]. The IGV, rotor and cavity are meshed with a structured grid generation tool named AutoGrid™ and is converted to an unstructured grid by the tool Hexpress™. The cavity is connected to the flow path of row 3 by full non-matching boundary interfaces (FNMB) at the inflow and outflow of the cavity. For the inlet conditions of the stage a boundary layer profile of the total pressure and total temperature is specified as well as an axial inflow and a turbulent intensity of 5%. For the outlet boundary different mass flows are imposed to change the working point of the whole stage. Second order central scheme and steady state simulations are carried out with only one periodic passage. All periodic boundaries are meshed using a full-matching approach. The turbulence model used for all calculations is the SARC model that is a modified version of the well-known and robust Spalart Allmaras turbulence model [6]. Moreover, the initialisation of each calculation is done by constant values of all necessary flow parameters for each row and a non-linear multigrid strategy is used to speed up the convergence of the CFD calculation. First, a grid study of the reference tandem stator without near-endwall modification is done at the design point of the compressor. Because of comparability the reference tandem stator is also meshed with a hybrid meshing approach used by the tool HexpressHybrid™. After a sufficient resolution of the mesh is found the same mesh setting are used for the tandem stator with near-endwall modifications. Additionally some refinements for the edges of the connecting regions are integrated as a second step to evaluate the impact of a higher resolution of the mesh near those areas. The mass-averaged loss coefficient $\overline{\overline{\omega}}|_{MM}$ is used as the parameter of interest for the grid study.

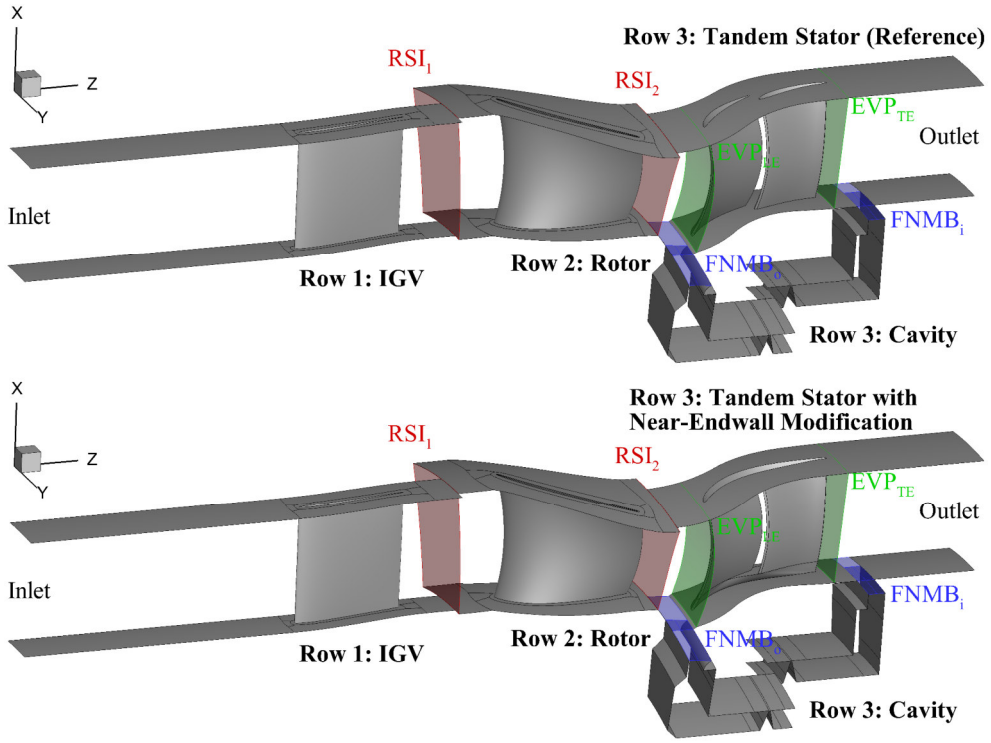

Figure 3. Numerical set up of the 1.5-low speed compressor with a tandem stator with (top) and without (bottom) near-endwall modification

The loss coefficient is calculated by equation 1 (appendix) between the two evaluation planes (EVP) that are placed five percent of the chord length upstream and downstream of the stator edges. Figure 4 is showing a decrease of the loss coefficient with an increase of nodes for the reference tandem stator. At approximately 23 million nodes for the whole stage, the loss coefficient of the reference tandem stator only changes by a delta of $3.61e^{-4}$, which is 100 time lower as the change between the two coarsest meshes. Additional refinements at the edges of the connecting region for the tandem stator with near end-endwall modification have no impact on the loss coefficient. At comparable mesh settings, the mesh of the modified geometry is 20% bigger as the reference one, which is based on the additional refinements at the connecting regions. The delta of the loss coefficient between both geometries is

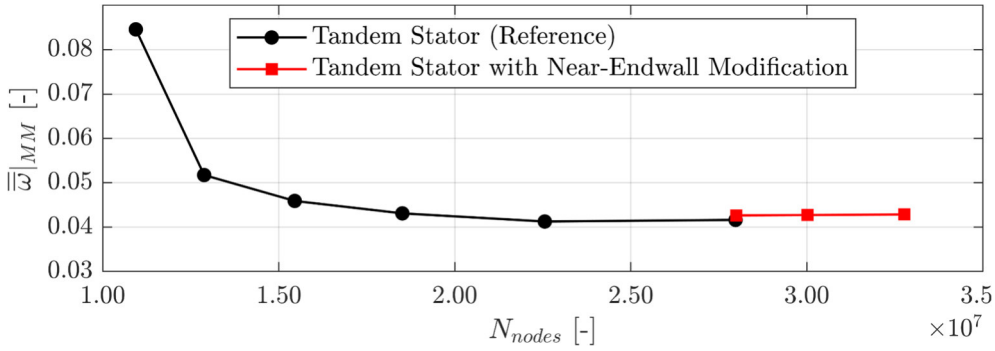

Figure 4. Grid independency of the loss coefficient for both unstructured hybrid meshes

$1.37e^{-3}$ which is lower than the impact of the mesh settings. The quality criteria of the final meshes for both geometries are in a good agreement and the convergence of the difference between the inlet and outlet mass flows is showing no oscillation for both configurations.

4. Numerical results

As mentioned before the performance parameters such as the loss coefficient ω, the pressure rise coefficient C_p, the turning $\Delta\beta$ and the axial velocity density ratio AVDR are calculated between the evaluation planes EVP_{LE} and EVP_{TE} of row 3. The characteristics of the tandem stator with and without near-endwall modification at different relative mass flows $\dot{m}/\dot{m}_{DP}$ are shown in figure 5. The losses of the tandem stator with near-endwall modification are shifted to higher values but at the limits of the working range the modified geometry shows similar losses compared to the reference tandem stator. The other performance parameters are showing a slight improvement for the near-endwall modification at higher mass flows but a deterioration at lower mass flows. The AVDR, which is representing the blockage of the stator, is showing a more constant behaviour over the operating range of the stage.

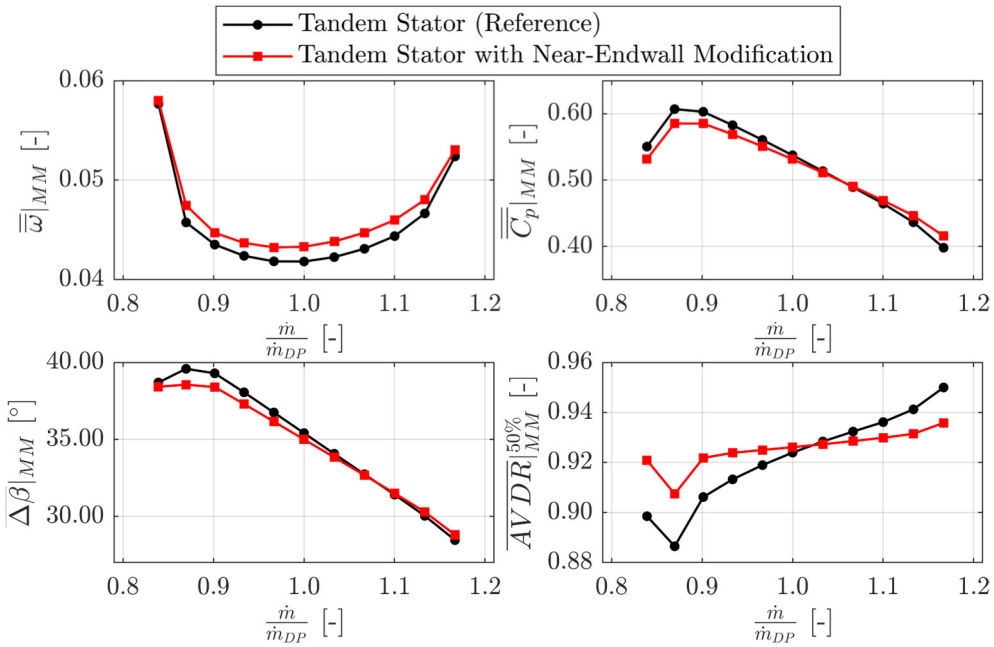

Figure 5. Mass-averaged performance parameters of row 3 at different operating points

To get a better understanding of those blade regions, which are responsible for the higher losses circumferential averaged radial distributions of the mass-averaged loss coefficient are shown at three different operating points (figure 6). At the design point ($\dot{m}/\dot{m}_{DP} = 1.00$) the near-endwall configuration is reducing the local maxima of the losses of the reference case at 10% and 90% span but at the same time new loss peaks appear at 20% and 80% span. The losses at midspan are also slightly increased. The same kind of redistribution of the losses over the span can be seen at the throttled condition of the compressor stage ($\dot{m}/\dot{m}_{DP} = 0.90$). Furthermore, the loss peaks are both increasing with the throttling and the positive effect of the near-endwall modification, which is the reduction of the local loss maxima, is weakened at the shroud and slightly strengthened at the hub. This reverse behaviour of the positive effect over the span is connected to the development of the local loss maxima of the reference tandem stator, which is also different at hub and shroud. At the hub the local losses of the reference case are increasing but at the shroud they are decreasing. For higher relative mass flows ($\dot{m}/\dot{m}_{DP} = 1.10$) an opposite behaviour is happening. On the one hand, the loss peaks at 20% and 80%

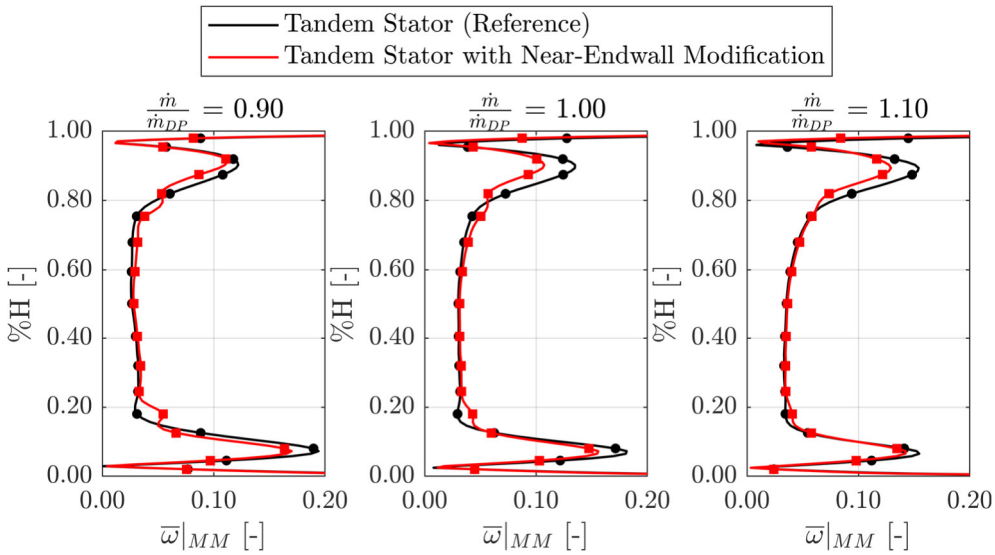

Figure 6. Mass-averaged radial distribution of the loss coefficient at different operating points

span are vanishing and on the other hand, the positive effect of the near-endwall configuration is switched between both endwalls. This also seems to be related to the development of the local loss maxima of the reference tandem stator that are increasing at the shroud and decreeing at the hub for the de-throttled case. The overall losses are higher for all working points because the redistribution of the losses seems to be not efficient over the span. However, the trend of the higher loss peaks at lower mass flows such as the lowering of big local loss maxima of the reference geometry can be figured out. The open question is which flow phenomena are triggering the local peaks as well as the reduction of the local loss maxima. To answer this question figure 7 is showing wall streamlines and contour of the friction coefficient c_f at the suction side and the hub of the reference tandem stator. Moreover, the contour of the absolute Mach number Ma is plotted at two different axial slices. One slice is the

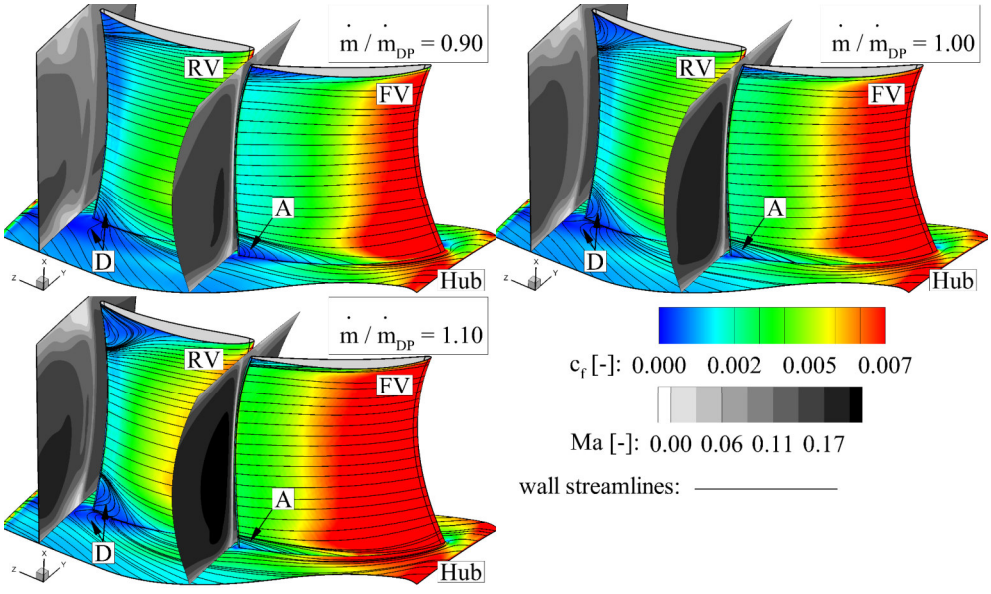

Figure 7. Wall streamlines and contour plot of the friction coefficient and the Mach number at different operating points for the tandem stator (reference)

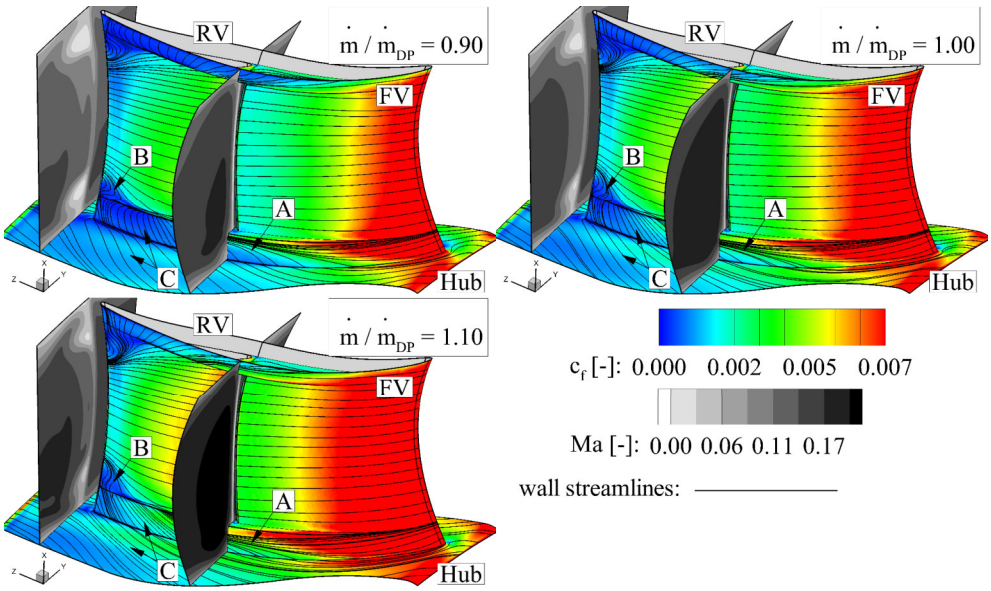

Figure 8. Wall streamlines and contour plot of the friction coefficient and the Mach number at different working points for the tandem stator with near-endwall modification

evaluation plane EVP_{TE} and the other is slice placed between the front and rear vane. The same depiction is used for the tandem stator with near endwall modification and can be seen in figure 8. The comparison between both geometries is showing that the loss peaks of the near-endwall modification at 20% and 80% span are related to areas of low momentum fluid downstream of the trailing edge, which are not present for the reference case. The area of low momentum fluid is caused by the fluid of the area C (figure 8), which is moving from the endwalls over the suction side of the single-profile segment and finally separating at the edge of the connecting surface. Moreover, a mixture of the separated fluid and the fluid, which is coming from the gap area of the connecting surface, is happening in area B. This mixture is causing some additional reversal flow at higher span positions and is increasing in size with decreeing relative mass flow. At lower mass flows and higher pressure ratios the slops of the wall streamlines at the suction side of the single-profile segment (area C) is higher. This is leading to an earlier separation, which is mainly triggering the higher loss peaks at lower mass flows. The reference tandem stator is showing lower friction coefficients and steeper wall streamlines near the trailing edge of the front vane (area A) at lower mass flows. This area of the front vane is slightly influenced by the

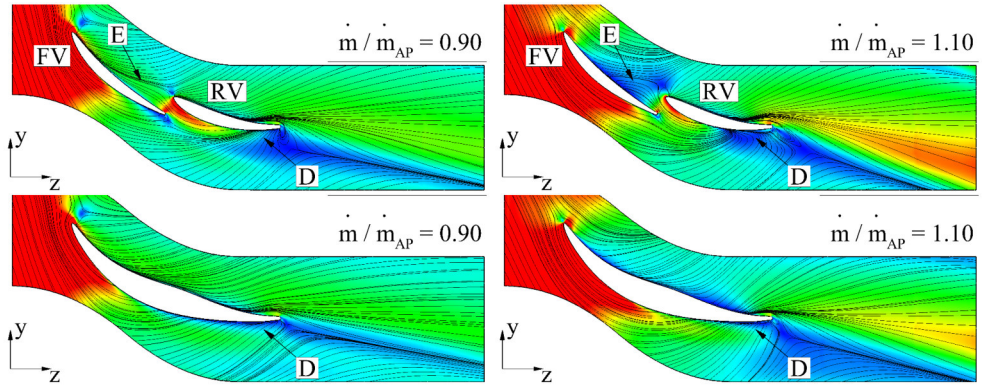

Figure 9. Wall streamlines and contour plot of the friction coefficient at the shroud surface

near-endwall configuration. With an increase of mass flow, the loading is shifted to the rear vane of the reference tandem stator. This causes the fluid to form a corner separation near the trailing edge of the rear vane (area B) as well as an increase of low momentum fluid at both endwalls downstream of the trailing edge. This corner separation and the area of low momentum fluid can be reduced with the introduction of the near-endwall modification. Figure 9 is representing the wall streamlines and the contour of the friction coefficient at the shroud surface for both geometries. Due to the removal of the gap flow and the upstream pressure effect of the second leading edge, no low energy fluid will be mixed to the crossflow at the trailing edge of the rear vane (area D) anymore. As the result, the corner separation can be reduced.

5. Conclusion and Outlook

The introduction of a tandem stator featuring a near-endwall modification including the description of the geometry generation process, the structure of the numerical set up as well as the first numerical comparison between the reference tandem stator and the modified geometry is presented. At the first view, the overall losses of the reference tandem stator could not be reached at all operating points. However, the near-endwall modification is able to achieve a bigger turning and static pressure rise at mass flow rates higher than the design point. This effect is primary triggered by the reduction of the corner separation at the rear vane of the reference tandem stator, which is only present at high mass flows. The geometry creation process allows designing and optimizing new geometries of the near-endwall modification for further steps. For example, the profiling and the height of the single-profile segment can be changed to reduce the separation of fluid at the edge of the connecting surface. This separation is the major reason for the higher losses of the new geometry. Additionally various reference tandem stators will be modified to the see the effect of load split between the front and rear vane on the impact of the near-endwall modification.

Acknowledgments

The present work was conducted at the chair of turbomachinery and flight propulsion of the Technical University of Munich.

6. Appendix

$$\bar{\bar{\omega}}|_{MM} = \frac{\bar{\bar{p}}_{t,EVP_{TE}}|_{MM} - \bar{\bar{p}}_{t,EVP_{LE}}|_{MM}}{0.5 \cdot \bar{\bar{\rho}}_{EVP_{LE}}|_{MM} \cdot \bar{\bar{c}}^2_{EVP_{LE}}|_{MM}} \tag{1}$$

$$\overline{\overline{C_p}}|_{MM} = \frac{\bar{\bar{p}}_{s,EVP_{TE}}|_{MM} - \bar{\bar{p}}_{s,EVP_{LE}}|_{MM}}{0.5 \cdot \bar{\bar{\rho}}_{EVP_{LE}}|_{MM} \cdot \bar{\bar{c}}^2_{EVP_{LE}}|_{MM}} \tag{2}$$

$$\overline{\overline{\Delta\beta}}|_{MM} = \bar{\bar{\beta}}_{EVP_{TE}}|_{MM} - \bar{\bar{\beta}}_{EVP_{LE}}|_{MM} \tag{3}$$

$$\overline{AVDR}|^{50\%}_{MM} = \frac{\bar{\rho}_{EVP_{TE}}|^{50\%}_{MM} \cdot \bar{c}_{z_{EVP_{TE}}}|^{50\%}_{MM}}{\bar{\rho}_{EVP_{LE}}|^{50\%}_{MM} \cdot \bar{c}_{z_{EVP_{LE}}}|^{50\%}_{MM}} \tag{4}$$

7. References

[1] Grieb H 2009 *Verdichter für Turbo-Flugtriebwerke* Springer-Verlag (Berlin Heidelberg)

[2] Wennerstrom A J 1990 *Highly Loaded Axial Flow Compressors: History and Current Developments* Journal of Turbomachinery Vol. 112(4): 567–578

[3] McGlumphy J, Wing-Fai N and Wellborn S R 2008 *3D Numerical Investigation of Tandem Airfoils for a Core Compressor Rotor* In ASME Turbo Expo 2008: Turbomachinery Technical Conf. and Exp., no. GT2008-50427 American Society of Mechanical Engineers ASME International (Berlin, Germany)

[4] Heinrich A, Tiedemann C and Peitsch D 2017 *Experimental Investigation of the Aerodynamics of Highly Loaded Tandem Vanes in a High-Speed Stator Cascade* In ASME Turbo Expo 2017: Turbomachinery Technical Conf. and Exp., no. GT2017-63235 American Society of Mechanical Engineers, ASME International (Charlotte, NC, USA)

[5] NUMECA International 2019 *Theory Guide FINE™/Open with OpenLabs™ 9.1*

[6] Shur M L, Strelets M K and Spalart P R 2000, *Turbulence Modeling in Rotating and Curved Channels: Assessing the Spalart-Shur Correction* AIAA Journal Vol. 38(5): 784-792